TUDelft

Delft University of Technology

Cooperative distributed predictive control for collision-free vehicle platoons

Zheng, Huarong ; Wu, Jun; Wu, Weimin; Negenborn, Rudy

Important note
To cite this publication, please use the final published version (if applicable).
Please check the document version above.

Cooperative distributed predictive control for collision-free vehicle platoons

Huarong Zheng[1], Jun Wu[1], Weimin Wu[1,*], Rudy R. Negenborn[2]

[1] The State Key Laboratory of Industrial Control Technology and Institute of Cyber-Systems and Control, Zhejiang University, Zheda Road 38, 310027, Hangzhou, China
[2] Department of Maritime and Transport Technology, Delft University of Technology, Mekelweg 2, 2628 CD, Delft, The Netherlands
* E-mail: wmwu@iipc.zju.edu.cn

Abstract: The rapidly developing computing and communication technologies improve the autonomy of individual vehicles on the one hand and facilitate the coordination among vehicles on the other. In the context of dynamic speed management, this paper considers a platoon of intelligent vehicles that are required to maintain desired inter-vehicle spaces and to respond to speed changes in a collision-free, stable and cooperative way. The platoon is modelled as a cascaded network with linear longitudinal vehicle dynamics, independent physical constraints, and coupling safety constraints. In the case of global information sharing, we first propose a centralized collision-free solution based on model predictive control that guarantees asymptotic platoon tracking of speed changes and satisfaction of system constraints during the transient process. A cooperative distributed approach is then further proposed based on the alternating direction method of multipliers resulting in a scheme involving communication only with the roadside infrastructure, e.g., the speed manager. Vehicles in a platoon conduct parallel computation while still achieving global optimal performance and coordination with respect to the collision avoidance constraints. Convergence properties of the distributed solutions are established for the concerned vehicle platoon problem. Simulation results show satisfactory platoon performance and demonstrate the effectiveness of the proposed algorithms.

1 Introduction

Large cities are benefiting from the widely implemented intelligent transport systems (ITS) that improve traffic safety, efficiency, and sustainability significantly. Vehicle platoons are connected vehicles that move with closer inter-vehicle spaces, and thus increase road throughput due to vehicle-to-vehicle (V2V) and vehicle-to-infrastructure (V2I) communication. Instead of the random and possible selfish human car-following behaviours, cooperative autonomous manoeuvring of vehicles in a platoon aims at system-wide economical and safety crucial goals preferably still retaining individual decision-making. Moreover, guaranteed platoon performance during both transient and asymptotic processes in varying traffic scenarios could make the platoon control problem even more complex.

Various technological aspects involved in the vehicle platoon problem have been considered in the literature. From both microscopic and macroscopic traffic perspectives, the positive and negative impacts of vehicle platoons on environment and moving jams are assessed by [1] [2]. These works confirm that properly designed car-following controllers contribute to higher road capacity and smoother traffic flows. For logistics applications, truck platoons are being tested on freeways due to the ability to reduce air drag and save fuel when driving close together. Fuel-optimal routes and reference speed profiles for lower-level controllers to track are calculated for truck platoons in [3]. Longitudinal vehicle control plays an important role in platoon behaviours and the research can be dated back to 1990s at PATH California [4]. In the one-dimensional longitudinal direction, different spacing policies, e.g., constant distance, constant time headway distance or other nonlinear speed dependent distances, result in different platoon control performance [5]. The constant distance spacing policy is used the most widely due to its simplicity. As a physically uncoupled chain system, the impact of different communication topologies is explored in [6] [7]. Information flow involved issues such packet loss or time delays are usually treated as disturbances. Robust control [8], event-trigger based [9], and network analysis [10] tools are usually applied to attenuate the influence

of disturbances. Most existing research requires V2V communications in a either predecessor-follower or predecessor-leader-follower, directional or bi-directional way. For scenarios where vehicle information is kept private among vehicles, coordinated decision-making could be challenging.

Principally, the vehicle platoon coordination problem can be solved centrally at the platoon level or locally at the vehicle level. However, distributed controllers are customarily designed for vehicle platoons due to the following reasons: *1)* platoon vehicles are physically distributed by nature; *2)* the inherent modularity in a distributed design facilitates possible split or merge platoon behaviours; *3)* local information is kept private to individual drivers; *4)* a distributed design is more robust to local platoon vehicle failures; *5)* distributed smaller local problems are computationally more efficient to solve. A highly relevant technology is the so-called cooperative adaptive cruise control (CACC) technology that autonomously maintains vehicle speed and distance to a preceding vehicle at certain values [11]. Mostly, a reference acceleration is calculated based on relative speed and distance information for the following vehicle. However, no overall platoon performance, e.g., optimality and stability, can be guaranteed for such CACC systems [2]. Different distributed platoon controllers that guarantee certain platoon performance under particular assumptions have been proposed. Based on H_∞ control, [6] [12] propose distributed state feedback controllers that guarantee robustness for vehicle platoons with different interaction topologies. No system constraints are accommodated. In [13], a primal-dual distributed computation scheme is proposed with consideration of physical and safety constraints. However, the connections among vehicles are treated as the distributed computation nodes rather than physically distributed vehicles. Moreover, asymptotic stability is only guaranteed for the unconstrained case. Model predictive control (MPC) has the advantages of handling conflicting objectives, constraints conveniently with inherent robustness and guaranteed closed-loop properties for certain classes of systems [14]. Distributed vehicle platoon or formation controllers based on MPC are proposed in [15] [16] [17]. Techniques are proposed for ensuring vehicle and platoon stability. While [15] and [16] only consider uncoupled physical constraints, [17] requires that each vehicle

solves the optimization problem for all the vehicles in the neighbourhood and invokes extra mechanism for coupled collision avoidance constraints. A compact solution to distributed control, guaranteed performance, and safety constraint satisfaction for vehicle platoons has not been seen.

For distributed MPC [18] with coupled state constraints, system properties are usually established by assuming that the deviations of trajectories from consecutive steps are small, ensured by compatibility [19], consistency [17] constraints or deviation penalties in cost functions [15] [16]. When assuming the deviations are bounded, robust approaches can also be applied [20] [21]. However, the aforementioned methods all sacrifice certain system optimality in order to achieve distributed control. In general, the iterative optimization frameworks such as dual decomposition [13] and the alternating direction method of multipliers (ADMM) [22] can achieve optimality close to the corresponding centralized problem, and thus realize cooperative distributed control. Dual decomposition and ADMM based distributed distributed MPC are compared in [23] and show that ADMM has better convergence properties. The decomposition-coordination procedure of ADMM has well established convergence properties [22] for certain type of problems. Applications of ADMM for distributed MPC are seen in communication networks to reduce congestions [24], networked road vehicles [25] and waterborne AGV transport systems [26]. Parallel computations that treat all networked nodes equally with guaranteed overall performance and satisfaction of coupling constraints are possible at the same time. However, applications of ADMM to vehicle platoons have not been discussed in the literature to date.

This paper proposes an ADMM-based cooperative distributed MPC controller for intelligent vehicle platoons that systematically guarantees both collision-free manoeuvres and platoon performance in terms of speed tracking and inter-vehicle space maintenance. Particularly, we consider a dynamic speed management scenario where vehicles in a platoon are required to respond to speed changes and maintain desired inter-vehicle distance with actual distances not smaller than a safety distance in both transient and asymptotic processes. Centralized and distributed solutions that need global and partial information sharing, respectively, are proposed with guaranteed closed-loop stability. Particularly, the distributed decision-making relies on communication only with the roadside infrastructure that acts as the coordinator in ADMM iterations. This contributes to a new and flexible information flow topology. Moreover, convergence properties for the distributed solution are established for the underlying vehicle platoon problem. Scenarios of accelerations and decelerations are simulated to illustrate the performance of the proposed algorithms. To the best of our knowledge, this is the first work that handles coupling collision avoidance constraints, constrained stability, and distributed decision-making with overall system optimality for vehicle platoons in a systematic way.

The remainder of this paper is organized as follows. We present the platoon control problem in the dynamic speed management scenario as well as the vehicle platoon dynamics for later controller design in Section 2. Then in Section 3, a cooperative centralized scheme based on MPC is first proposed and the closed-loop performance is studied. Distributed decision-making based on ADMM with convergence analysis is proposed in Section 4. In Section 5, simulation experiments and results are discussed, followed by concluding remarks and future research in Section 6.

2 Problem statement and vehicle platoon dynamics

2.1 Problem statement

The decision-making with intelligent vehicles is typically categorised into hierarchical levels [11] for managing traffic on different spatial and temporal scales, as shown in Figure 1. The network layer uses route guidance to distribute the traffic in a large road network. The link layer controls the speed and the size of any existing platoons on a specific road segment. Vehicle layers then compute
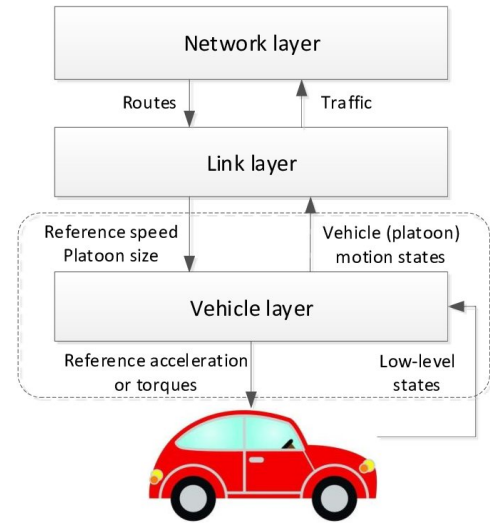

Fig. 1: Typical ITS decision-making levels with intelligent vehicles.

proper accelerations or lower level torques/power to track the reference speed. For completeness, the following assumptions are made regarding the cooperative distributed platoon problem considered at the vehicle layer: *1*) Platoon vehicles are considered as mass points, and detailed vehicle powertrain dynamics including engine, driveline, brake systems, etc. are not considered. Therefore, the reference accelerations from the vehicle layer could be implemented by low-level actuators perfectly with no inertial delay. *2*) All vehicles are equipped on-board with sensors, micro-computers and communication devices to measure system states, solve local problems and communicate with other platoon vehicles. Moreover, zero sensor errors and communication delays are assumed for these devices. *3*) Vehicles are on a straight way and the lateral manoeuvres are governed by either human drivers or lateral stability controllers [27].

The link and vehicle layers are connected by V2I communication in the dynamic speed scenario. Specifically, we consider a fixed number of n intelligent vehicles moving as a platoon that receives dynamic reference speeds $v_0(k)$ from the road-side link every several minutes, as shown in Figure 2. The discrete-time step k relates to the continuous-time t as $t = kT_s$ with T_s as the sampling time. The longitudinal platoon formation is guaranteed by a desired constant inter-vehicle space, d_s. Furthermore, an actual minimum distance, $d_{\min}$, is imposed to avoid rear-end collisions. The overall platoon control goals are to maintain the constant space formation and to track the dynamic reference speeds in a cooperative and stable way while guaranteeing safety in both transient and asymptotic processes.

2.2 Vehicle platoon dynamics

Without loss of generality, we assume homogeneous longitudinal dynamics for simplicity for all vehicles $p = 1, 2, \ldots, n$ in the platoon. For each vehicle p, define $(s_p(k), v_p(k))$ as the discrete-time system states, i.e., the position and speed, and $a_p(k)$ as the discrete-time system input, i.e., the acceleration. Longitudinal vehicle dynamics are then described by the widely used double-integrator [2] [12] [13] [28] as:

$$\boldsymbol{x}_p(k+1) = \boldsymbol{A}_p\boldsymbol{x}_p(k) + \boldsymbol{B}_p u_p(k), \qquad (1)$$

with $\boldsymbol{x}_p(k) = [s_p(k), v_p(k)]^T$, $u_p(k) = a_p(k)$, state matrix $\boldsymbol{A} = \begin{bmatrix} 1 & T_s \\ 0 & 1 \end{bmatrix}$, and input matrix $\boldsymbol{B} = \begin{bmatrix} T_s^2/2 \\ T_s \end{bmatrix}$.

Due to physical limitations on speeds and accelerations, vehicle manoeuvres are also confined by constraints on states and control inputs:

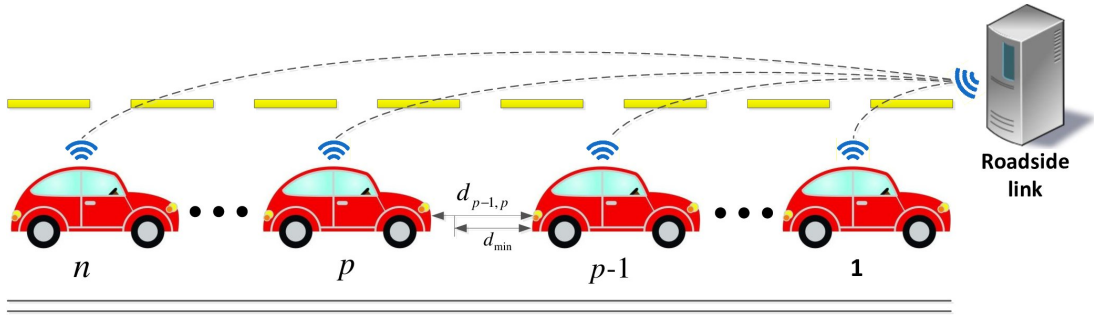$$v_{\min} \leq v_p(k) \leq v_{\max}, \qquad (2)$$

Fig. 2: Vehicle platoon in a dynamic speed management scenario.

$$a_{\min} \le a_p(k) \le a_{\max}, \tag{3}$$

where $v_{\min}$, $v_{\max}$, $a_{\min}$, and $a_{\max}$ are specified bounds on vehicle longitudinal speed and acceleration.

To avoid possible collisions, the actual distances between consecutive vehicles are required to satisfy

$$s_{p-1}(k) - s_p(k) \ge d_{\min} \tag{4}$$

with $d_{\min} = L + \tau v_p(k) - \left(v_{\max}^2 - v_{\min}^2\right)/2$ that is dependent on vehicle length L, mechanical reaction time $\tau \ge T_s$, and the speed bounds. Note that vehicle $p-1$ represents the vehicle in front of vehicle p.

Vehicles keep a platoon formation by moving at the same speed and maintaining the desired space between adjacent vehicles. For the tracking problem with reference speed $v_0(k)$, we define a virtual reference trajectory $\boldsymbol{x}_0(k) = [s_0(k), v_0(k)]^T$ with $s_0(k)$ being the reference position, and $\boldsymbol{x}_0(k+1) = \boldsymbol{A}x_0(k)$ for the time period when the dynamic reference speed is not updated. Further define the error states for $p = 1, 2, \ldots, n$ as:

$$\boldsymbol{z}_p(k) = \left[\begin{array}{c} s_{p0}(k) \\ v_{p0}(k) \end{array}\right] = \left[\begin{array}{c} s_p(k) - s_0(k) + (p-1)d_s \\ v_p(k) - v_0(k) \end{array}\right]. \tag{5}$$

Then, the error system dynamics are:

$$\boldsymbol{z}_p(k+1) = \boldsymbol{A}_p \boldsymbol{z}_p(k) + \boldsymbol{B}_p u_p(k). \tag{6}$$

Correspondingly, speed constraints (2) and safety constraints (4) are transformed as:

$$v_{\min} - v_0(k) \le v_{p0}(k) \le v_{\max} - v_0(k), \tag{7}$$

and

$$s_{(p-1)0}(k) - s_{p0}(k) \ge d_s + L + \tau\left(v_{p0}(k) + v_0(k)\right) - \left(v_{\max}^2 - v_{\min}^2\right)/2, \tag{8}$$

respectively.

Assumption 1. *The reference speed $v_0(k)$ satisfies the vehicle speed constraints (2), i.e., $v_{\min} \le v_0(k) \le v_{\max}$.*

For each vehicle p, denote the error state constraint set due to (7) as $\mathcal{Z}_p(k)$, and the input constraint set due to (3) as $\mathcal{U}_p$. For the vehicle platoon, denote the coupling constraint set due to (8) as $\mathcal{Z}_c(k)$. Then, under Assumption 1, the sets $\mathcal{Z}_p(k)$, $\mathcal{U}_p$ and $\mathcal{Z}_c(k)$ are all closed convex and contain the origin in their interior. The coupling collision avoidance constraints (8) impede individual solutions to the vehicle platoon problem. Centralized and distributed approaches are proposed in the next section to achieve the control goals stated at the beginning of this section.

3 Centralized platoon control with stability

We propose a centralized solution first in this section based on MPC, and explore the closed-loop properties that guarantee transient and asymptotic performance. At each time step k, MPC solves an open-loop constrained optimization problem over a finite time prediction horizon N based on current system states $\boldsymbol{z}_p(k)$. The first optimal control input is applied to the system over $[kT_s, (k+1)T_s]$. At time step $k+1$, the optimization problem is solved using new measurements over a shifted prediction horizon. We next present how the receding horizon centralized platoon problem at step k is formulated.

$$\min_{\boldsymbol{U}(k)} \; J_{\sum}\left(\boldsymbol{z}(k), \boldsymbol{U}(k)\right) = \sum_{p=1}^{n} J_p(\boldsymbol{z}_p(k), \boldsymbol{U}_p(k)) \tag{9}$$

with

$$J_p(\boldsymbol{z}_p(k), \boldsymbol{U}_p(k)) = \\ \|\boldsymbol{z}_p(N|k)\|_{\boldsymbol{P}_p} + \sum_{i=0}^{N-1} \|\boldsymbol{z}_p(i|k)\|_{\boldsymbol{Q}} + \|u_p(i|k)\|_{\boldsymbol{R}} \tag{10}$$

subject to

$$\boldsymbol{z}_p(i+1|k) = \boldsymbol{A}_p\boldsymbol{z}_p(i|k) + \boldsymbol{B}_p u_p(i|k), \\ i = 0, \ldots, N-1, p = 1, \ldots, n \tag{11}$$

$$\boldsymbol{z}_p(i|k) \in \mathcal{Z}_p(k), \; i = 0, \ldots, N-1, p = 1, \ldots, n \tag{12}$$

$$u_p(i|k) \in \mathcal{U}_p, \; i = 0, \ldots, N-1, p = 1, \ldots, n \tag{13}$$

$$\boldsymbol{z}_p(N|k) \in \mathcal{Z}_p^f(k), \; p = 1, \ldots, n \tag{14}$$

$$\boldsymbol{z}_p(0|k) = \boldsymbol{z}_p(k), \; p = 1, \ldots, n \tag{15}$$

$$\left(\boldsymbol{z}_1(i|k), \ldots, \boldsymbol{z}_n(i|k)\right) \in \mathcal{Z}_c(k), \; i = 0, \ldots, N-1 \tag{16}$$

$$\left(\boldsymbol{z}_1(N|k), \ldots, \boldsymbol{z}_n(N|k)\right) \in \mathcal{Z}_c^f(k), \tag{17}$$

where $i|k$ stands for the ith prediction step at time step k, and hereby, if contextually clear, $i = 0, \ldots, N-1$. The predicted error states $\boldsymbol{z}_p(i|k)$ in (11) are defined based on (5) with the reference trajectory over N as

$$\left[\begin{array}{c} s_0(i+1|k) \\ v_0(i+1|k) \end{array}\right] = \boldsymbol{A}\left[\begin{array}{c} s_0(i|k) \\ v_0(i|k) \end{array}\right]$$

and $[s_0(0|k), v_0(0|k)]^{\mathrm{T}} = [s_0(k), v_0(k)]^{\mathrm{T}}$. For notational simplicity, define capitalized characters $\boldsymbol{Z}_p(k) \in \mathcal{R}^{2\times(N+1)}$ and $\boldsymbol{U}_p^T(k) \in \mathcal{R}^N$ as the predicted state and input trajectories over N for vehicle p, respectively, and $\boldsymbol{Z}(k) \in \mathcal{R}^{2n\times(N+1)}$ and $\boldsymbol{U}(k) \in \mathcal{R}^{n\times N}$ as the predicted state and input trajectories over N for the entire platoon, respectively. The platoon initial state has also been compactly denoted as $\boldsymbol{z}(k) = \left[\boldsymbol{z}_1^T(k), \ldots, \boldsymbol{z}_n^T(k)\right]^T \in \mathcal{R}^{2n}$. The total cost function $J_{\sum}\left(\boldsymbol{z}(k), \boldsymbol{U}(k)\right)$ is a summation of costs over individual vehicle costs, and the individual vehicle cost (10) consists of the stage costs and the terminal cost minimizing the tracking

errors and control input efforts. The symbol $\|\boldsymbol{z}_p(i|k)\|_{\boldsymbol{Q}}$ stands for the weighted 2-norm, i.e., $\boldsymbol{z}_p^T(i|k)\boldsymbol{Q}\boldsymbol{z}_p(i|k)$. The weight matrices satisfy $\boldsymbol{Q} = \boldsymbol{Q}^T \succ 0$, $\boldsymbol{R} = \boldsymbol{R}^T \succ 0$, and $\boldsymbol{P}_p \succ 0$. The set of constraints can be categorized into independent constraints (11) – (15) and coupling constraints (16) – (17). In addition, $\mathcal{Z}_p^f(k)$ and $\mathcal{Z}_c^f(k)$ denote terminal constraint sets.

In general, the closed-loop system stability, i.e., the convergence of the tracking errors $\boldsymbol{z}_p(k)$ to the origin, is not guaranteed. Following standard MPC results [14], we next briefly discuss how the terminal weight matrix $\boldsymbol{P}_p$ and the terminal constraint sets $\mathcal{Z}_p^f(k)$ and $\mathcal{Z}_c^f(k)$ are designed to ensure the closed-loop stability of the centralized platoon problem.

For all vehicles $p = 1, \ldots, n$, set $\boldsymbol{P}_p$ as the solution to the infinite horizon algebraic Riccati equation, i.e.,

$$\boldsymbol{P}_p = \boldsymbol{Q} + \boldsymbol{A}_p^T \boldsymbol{P}_p \boldsymbol{A}_p - \boldsymbol{A}_p^T \boldsymbol{P}_p \boldsymbol{B}_p \left(\boldsymbol{R} + \boldsymbol{B}_p^T \boldsymbol{P}_p \boldsymbol{B}_p \right)^{-1} \boldsymbol{B}_p^T \boldsymbol{P}_p \boldsymbol{A}_p.$$

Consider the closed-loop error dynamics for the linear time-invariant system (6), i.e., $\boldsymbol{z}_p(k+1) = (\boldsymbol{A}_p + \boldsymbol{B}_p \boldsymbol{F}_p) \boldsymbol{z}_p(k)$ where $\boldsymbol{F}_p \in \mathcal{R}^{1\times 2}$ is the corresponding unconstrained Linear Quadratic Regulator (LQR) feedback gain as

$$\boldsymbol{F}_p = -\left(\boldsymbol{R} + \boldsymbol{B}_p^T \boldsymbol{P}_p \boldsymbol{B}_p \right)^{-1} \boldsymbol{B}_p^T \boldsymbol{P}_p \boldsymbol{A}_p \qquad (18)$$

Then, $\mathcal{Z}_p^f(k)$ is chosen as the maximal positive invariant set [29] for the closed-loop system $\boldsymbol{z}_p(k+1) = (\boldsymbol{A}_p + \boldsymbol{B}_p \boldsymbol{F}_p) \boldsymbol{z}_p(k)$ with respect to state constraint set on $\boldsymbol{z}_p(k)$:

$$\begin{bmatrix} 0 & 1 \\ 0 & -1 \\ f_p^1 & f_p^2 \\ -f_p^1 & -f_p^2 \end{bmatrix} \boldsymbol{z}_p(k) \le \begin{bmatrix} v_{\max} - v_0(k) \\ -v_{\min} + v_0(k) \\ a_{\max} \\ -a_{\max} \end{bmatrix},$$

where f_p^1, f_p^2 are the elements of $\boldsymbol{F}_p$, i.e., $\boldsymbol{F}_p = \left[f_p^1, f_p^2 \right]$.

Regarding $\mathcal{Z}_c^f(k)$, since all the vehicle states are coupled in the collision avoidance constraints, we consider the platoon closed-loop error dynamics

$$\boldsymbol{z}(k+1) = (\boldsymbol{A} + \boldsymbol{B}\boldsymbol{F}) \boldsymbol{z}(k) \qquad (19)$$

with $\boldsymbol{A} = \text{blockdiag}(\boldsymbol{A}_1, \ldots, \boldsymbol{A}_n)$, $\boldsymbol{B} = \text{blockdiag}(\boldsymbol{B}_1, \ldots, \boldsymbol{B}_n)$, and $\boldsymbol{F} = \text{blockdiag}(\boldsymbol{F}_1, \ldots, \boldsymbol{F}_n)$. Then, $\mathcal{Z}_c^f(k)$ is chosen as the maximal positive invariant set for (19) with respect to the coupling constraint set on $\boldsymbol{z}(k)$:

$$\boldsymbol{C}\boldsymbol{z}(k) \le \boldsymbol{D} \qquad (20)$$

with the ith row of the coupling matrix $\boldsymbol{C} \in \mathcal{R}^{(n-1)\times 2n}$ being $\boldsymbol{C}_i = \left[\boldsymbol{0}_{1\times 2(i-1)}, -1, 0, 1, -\tau, \boldsymbol{0}_{1\times 2(n-i-1)} \right]$ and $\boldsymbol{D} = -\left(d_s + L + \tau v_0(k) - \left(v_{\max}^2 - v_{\min}^2 \right)/2 \right) \boldsymbol{1}_{(n-1)\times 1}$.

The above design of the terminal invariant sets $\mathcal{Z}_p^f(k)$, $\mathcal{Z}_c^f(k)$ and the terminal cost $\|\boldsymbol{z}_p(N|k)\|_{\boldsymbol{P}_p}$ will guarantee that

$$J_{\sum} \left(\boldsymbol{A}\boldsymbol{z}(k) + \boldsymbol{B}\boldsymbol{U}^*(k), \boldsymbol{U}^*(k+1) \right) - J_{\sum} \left(\boldsymbol{z}(k), \boldsymbol{U}^*(k) \right)$$

$$\le -\left(\sum_{p=1}^n \|\boldsymbol{z}_p(k)\|_{\boldsymbol{Q}} + \|u_p^*(k)\|_{\boldsymbol{R}} \right) < 0$$

which establishes the stability property of the centralized platoon problem (9) – (17). The closed-loop optimal trajectories $\boldsymbol{z}(k)$ are ensured to be driven towards the origin. Interested readers are referred to [14] for more stability proof details with the above design.

As can be seen from (19) and (20), the coupling collision avoidance constraints as well as calculation of the corresponding terminal constraint sets in the centralized platoon problem require the knowledge on all vehicle dynamics and trajectories. We next propose a distributed approach that enables vehicle parallel computation and retains the independence of platoon vehicles.

4 Cooperative distributed control and convergence analysis

For the vehicle platoon problem in the dynamic speed management scenario as defined in Section 2, vehicles have independent dynamics, objectives and physical constraints. However, the distance and speed dependent safety constraints that impose a minimal inter-vehicle space prohibit individual vehicle decision-making. This section proposes cooperative distributed controllers that ensure parallel local computation, satisfaction of coupling constraints, and global optimality at the same time based on the iterative decomposition-coordination procedure of ADMM [22]. Convergence of the iterations is also analysed exploring features of the vehicle platoon problem under concern.

4.1 Cooperative distributed formulation based on ADMM

At time step k, for all vehicles p in the platoon, we introduce a copy of the predicted error state variables $\boldsymbol{Z}_p(k)$ as $\tilde{\boldsymbol{Z}}_p(k)$. Define the coupling safety constraints (16) and the corresponding coupling terminal constraints (17) on $\tilde{\boldsymbol{z}}_p(i|k), i = 0, \ldots, N-1$ and $\tilde{\boldsymbol{z}}_p(N|k)$, respectively, then (16) and (17) can be rewritten using indicator functions as:

$$\mathcal{I}_{\mathcal{Z}_c}\left(\tilde{\boldsymbol{z}}_1(i|k), \ldots, \tilde{\boldsymbol{z}}_n(i|k) \right) \qquad (21)$$

$$= \begin{cases} 0, & \text{for } (\tilde{\boldsymbol{z}}_1(i|k), \ldots, \tilde{\boldsymbol{z}}_n(i|k)) \in \mathcal{Z}_c(k) \\ \infty, & \text{otherwise}, \end{cases}$$

for $i = 0, \ldots, N-1$, and

$$\mathcal{I}_{\mathcal{Z}_c^f}\left(\tilde{\boldsymbol{z}}_1(N|k), \ldots, \tilde{\boldsymbol{z}}_n(N|k) \right) \qquad (22)$$

$$= \begin{cases} 0, & \text{for } (\tilde{\boldsymbol{z}}_1(N|k), \ldots, \tilde{\boldsymbol{z}}_n(N|k)) \in \mathcal{Z}_c^f(k) \\ \infty, & \text{otherwise}, \end{cases}$$

The centralized platoon problem (9) – (17) is then equal to:

$$\min_{\boldsymbol{U}(k)} \sum_{p=1}^n J_p(\boldsymbol{z}_p(k), \boldsymbol{U}_p(k)) + \mathcal{I}_{\mathcal{Z}_c}(k) + \mathcal{I}_{\mathcal{Z}_c^f}(k) \qquad (23)$$

subject to (11) – (14) and

$$\boldsymbol{Z}_p(k) = \tilde{\boldsymbol{Z}}_p(k). \qquad (24)$$

for $p = 1, \ldots, n$. We further relax (24) by introducing the augmented Lagrangian as:

$$\mathcal{L}_\rho(k) = \sum_{p=1}^n \left\{ J_p(\boldsymbol{z}_p(k), \boldsymbol{U}_p(k)) + \boldsymbol{\lambda}_p^T(k) \left(\boldsymbol{Z}_p(k) - \tilde{\boldsymbol{Z}}_p(k) \right) \right.$$

$$\left. + \frac{\rho}{2} \left\| \boldsymbol{Z}_p(k) - \tilde{\boldsymbol{Z}}_p(k) \right\|_2^2 \right\} + \mathcal{I}_{\mathcal{Z}_c}(k) + \mathcal{I}_{\mathcal{Z}_c^f}(k) \quad (25)$$

where $\boldsymbol{\lambda}_p(k) \in \mathcal{R}^{2\times N_p}$ is the dual variable with respect to (24) and $\rho > 0$ is the augmented Lagrangian parameter. Observing that the first part of (25) as well as constraints (11) – (14) are separable for each vehicle p, we introduce a platoon coordinator, e.g., the link speed manager, for evaluating the coupling indicator functions, and we decompose the centralized problem following ADMM decomposition-coordination procedures. The coordinator then takes care of the collision avoidance constraints updating $\tilde{\boldsymbol{Z}}_p(k)$ while vehicles in the platoon are able to solve local problems updating $\boldsymbol{Z}_p(k)$ in a parallel way. Consensus between the coordinator and individual vehicles is achieved via iteratively adjusting the dual variable.

Specifically, the cooperative distributed platoon problem based on ADMM at each iteration $j = 0, 1, \ldots,$ consists of the following three steps with initial values $\boldsymbol{\lambda}_p^0(k)$ and $\tilde{\boldsymbol{Z}}_p^0(k)$:

Algorithm 1 Local problem: processed in parallel by all vehicles p

1: initializes $\boldsymbol{\lambda}_p^0(k)$ and $\tilde{\boldsymbol{Z}}_p^0(k)$;
2: **loop**
3:     computes $\boldsymbol{Z}_p^{j+1}(k)$ as (26);
4:     sends $\boldsymbol{Z}_p^{j+1}(k)$ and $\boldsymbol{\lambda}_p^j(k)$ to the coordinator;
5:     **repeat**
6:       wait;
7:     **until** $\tilde{\boldsymbol{Z}}_p^{j+1}(k)$ arrive;
8:     computes $\boldsymbol{\lambda}_p^{j+1}(k)$ as (28), and $j+1 \rightarrow j$;
9: **end loop**

Algorithm 2 Coordinator problem: processed by the coordinator

1: **repeat**
2:     **repeat**
3:       wait;
4:     **until** $\boldsymbol{Z}_p^{j+1}(k)$ and $\boldsymbol{\lambda}_p^j(k)$ arrive;
5:     computes $\tilde{\boldsymbol{Z}}_p^{j+1}(k)$ as (27);
6:     broadcasts $\tilde{\boldsymbol{Z}}_p^{j+1}(k)$ to all vehicles p;
7: **until** Stopping criteria are met.

Step 1: each vehicle p solves the following local problem and updates $(\boldsymbol{U}_p(k), \boldsymbol{Z}_p(k))$:

$$\left(\boldsymbol{U}_p^{j+1}(k), \boldsymbol{Z}_p^{j+1}(k)\right) = \arg\min J_p(\boldsymbol{z}_p(k), \boldsymbol{U}_p(k))$$
$$+ \boldsymbol{\lambda}_p^j(k)^T \left(\boldsymbol{Z}_p(k) - \tilde{\boldsymbol{Z}}_p^j(k)\right) + \frac{\rho}{2} \left\| \boldsymbol{Z}_p(k) - \tilde{\boldsymbol{Z}}_p^j(k) \right\|_2^2 \quad (26)$$

subject to (11) – (14). Note that since platoon vehicles are modeled as linear double-integrator (11), local problems (26) in Step 1 are all tractable and can be solved sufficiently fast by commercial solvers. The updated $\boldsymbol{Z}_p^{j+1}(k)$ is sent to the coordinator.

Step 2: with $\boldsymbol{Z}_p^{j+1}(k)$, the platoon coordinator solves the following problem and updates $\tilde{\boldsymbol{Z}}_p(k)$:

$$\tilde{\boldsymbol{Z}}_p^{j+1}(k) = \arg\min \mathcal{I}_{\mathcal{Z}_c}(k) + \mathcal{I}_{\mathcal{Z}_c^f}(k) + \quad (27)$$
$$\sum_{p=1}^n \left\{ \boldsymbol{\lambda}_p^j(k)^T \left(\boldsymbol{Z}_p^{j+1}(k) - \tilde{\boldsymbol{Z}}_p(k)\right) + \frac{\rho}{2} \left\| \boldsymbol{Z}_p^{j+1}(k) - \tilde{\boldsymbol{Z}}_p(k) \right\|_2^2 \right\}.$$

The updated $\tilde{\boldsymbol{Z}}_p^{j+1}(k)$ is then sent back to all the platoon vehicles.

Step 3: each vehicle p updates dual variables $\boldsymbol{\lambda}_p(k)$ based on $\boldsymbol{\lambda}_p^j(k)$, $\boldsymbol{Z}_p^{j+1}(k)$ and $\tilde{\boldsymbol{Z}}_p^{j+1}(k)$:

$$\boldsymbol{\lambda}_p^{j+1}(k) = \boldsymbol{\lambda}_p^j(k) + \rho \left(\boldsymbol{Z}_p^{j+1}(k) - \tilde{\boldsymbol{Z}}_p^{j+1}(k)\right). \quad (28)$$

The iterations continue until stopping criteria as specified next are achieved.

Note that the computations in *Step 1* and *Step 3* can be carried out in parallel by all the vehicles. The coordinator problem at *Step 2* can be further written into the Euclidean projections of $(\tilde{\boldsymbol{z}}_1(i|k), \ldots, \tilde{\boldsymbol{z}}_n(i|k))$, $i = 0, \ldots, N-1$ and $(\tilde{\boldsymbol{z}}_1(N|k), \ldots, \tilde{\boldsymbol{z}}_n(N|k))$ onto $\mathcal{Z}_c(k)$ and $\mathcal{Z}_c^f(k)$, respectively, which are implemented as:

$$\tilde{\boldsymbol{Z}}_p^{j+1}(k) = \arg\min \sum_{p=1}^n \left\| \tilde{\boldsymbol{Z}}_p(k) - \left(\boldsymbol{Z}_p^{j+1}(k) + \boldsymbol{\lambda}_p^{j+1}(k)/\rho\right) \right\|_2^2 \quad (29)$$

subject to (16) – (17).

The overall cooperative distributed algorithm is illustrated as Algorithm 1 that will be carried out locally by all platoon vehicles and Algorithm 2 that will be carried out by the coordinator link.

4.2   Convergence analysis and stopping criteria

We next show that the distributed platoon problem iteratively processed by Algorithm 1 and Algorithm 2 will achieve convergence as $j \rightarrow \infty$.

Firstly, for all vehicles p, define the local constraint set due to $\mathcal{Z}_p(k)$, $\mathcal{U}_p(k)$ and $\mathcal{Z}_p^f(k)$ as $\mathcal{C}_p(k)$, then the local cost functions can be written as $J_p(\boldsymbol{z}_p(k), \boldsymbol{U}_p(k)) + I_{\mathcal{C}_p}(k)$ with $I_{\mathcal{C}_p}(k)$ being the indicator function of $(\boldsymbol{z}_p(k), \boldsymbol{U}_p(k))$ over $\mathcal{C}_p(k)$ that equals zero for $(\boldsymbol{z}_p(k), \boldsymbol{U}_p(k)) \in \mathcal{C}_p(k)$ and ∞ otherwise.

Lemma 1. *Local and coordinator cost functions $J_p(\boldsymbol{z}_p(k), \boldsymbol{U}_p(k)) + I_{\mathcal{C}_p}(k)$ and $\mathcal{I}_{\mathcal{Z}_c}(k) + \mathcal{I}_{\mathcal{Z}_c^f}(k)$ are closed, proper and convex.*

Proof: Under Assumption 1, $\mathcal{Z}_p(k)$, $\mathcal{U}_p(k)$ and $\mathcal{Z}_c(k)$ are all closed convex and contain the origin in their interior. Then, the indicator functions are all closed, proper and convex. For $J_p(\boldsymbol{z}_p(k), \boldsymbol{U}_p(k))$ in the form of (10), it can rewritten as:

$$J_p(\boldsymbol{z}_p(k), \boldsymbol{U}_p(k)) = \boldsymbol{U}_p^T(k) \left(\boldsymbol{\Pi}^T \bar{\boldsymbol{Q}} \boldsymbol{\Pi} + \bar{\boldsymbol{R}} \right) \boldsymbol{U}_p(k) + \quad (30)$$
$$2\boldsymbol{z}_p^T(k) \left(\boldsymbol{\Gamma}^T \bar{\boldsymbol{Q}} \boldsymbol{\Pi} \right) \boldsymbol{U}_p(k) + \boldsymbol{z}_p^T(k) \left(\boldsymbol{\Gamma}^T \bar{\boldsymbol{Q}} \boldsymbol{\Gamma} \right) \boldsymbol{z}_p(k)$$

with $\bar{\boldsymbol{Q}} = \text{blockdiag}(\boldsymbol{Q}, \ldots, \boldsymbol{Q}, \boldsymbol{P}_p)$, $\bar{\boldsymbol{R}} = \text{blockdiag}(\boldsymbol{R}, \ldots, \boldsymbol{R})$, and $\boldsymbol{\Gamma}$, $\boldsymbol{\Pi}$ being the concatenated state and input matrices, respectively, as

$$\boldsymbol{\Gamma} = \begin{bmatrix} I \\ A \\ \vdots \\ \vdots \\ A^N \end{bmatrix}, \boldsymbol{\Pi} = \begin{bmatrix} 0 & \cdots & \cdots & 0 \\ B & 0 & \cdots & 0 \\ AB & \ddots & \ddots & \vdots \\ \vdots & \ddots & \ddots & \vdots \\ A^{N-1}B & \cdots & \cdots & B \end{bmatrix}$$

Consider $\boldsymbol{Q} \succ 0$, $\boldsymbol{R} \succ 0$ and $\boldsymbol{P}_p \succ 0$, we have $\left(\boldsymbol{\Pi}^T \bar{\boldsymbol{Q}} \boldsymbol{\Pi} + \bar{\boldsymbol{R}} \right) \succ 0$. Therefore, $J_p(\boldsymbol{z}_p(k), \boldsymbol{U}_p(k))$ is strongly convex, and closed, proper. $\square$

Lemma 2. *The unaugmented Lagrangian $\mathcal{L}_0(k)$ (with $\rho = 0$) of (25) has a saddle point.*

Proof: Since the constrained sets $\mathcal{C}_p(k)$ are with nonempty relative interior, the Slater's condition holds. Besides, since $J_p(\boldsymbol{z}_p(k), \boldsymbol{U}_p(k))$ is strongly convex, there exists a unique optimal solution $\boldsymbol{U}_p^*(k)$, and the strong duality holds so that the dual problem $\sup_{\boldsymbol{\lambda}} \inf_{\boldsymbol{U}_p(k)} \mathcal{L}_0(k)$ has an optimal solution $\boldsymbol{\lambda}^*(k)$. Therefore, $\left(\boldsymbol{U}_p^*(k), \boldsymbol{\lambda}^*(k) \right)$ is a saddle point of $\mathcal{L}_0(k)$, i.e.,

$$\mathcal{L}_0 \left(\boldsymbol{U}_p^*(k), \boldsymbol{\lambda}_p(k) \right) \leqslant \mathcal{L}_0 \left(\boldsymbol{U}_p^*(k), \boldsymbol{\lambda}_p^*(k) \right) \leqslant \mathcal{L}_0 \left(\boldsymbol{U}_p(k), \boldsymbol{\lambda}_p^*(k) \right).$$

$\square$

Proposition 1 (Convergence of the distributed platoon problem). With Lemma 1 and Lemma 2, the following convergence is achieved as iteration $j \rightarrow \infty$:

1. Primal feasibility, i.e., $\boldsymbol{Z}_p^j(k) \rightarrow \tilde{\boldsymbol{Z}}_p^j(k)$ for all vehicles p;
2. Objective convergence, i.e., the objective function $J_{\sum}(\boldsymbol{z}(k), \boldsymbol{U}(k))$ approaches the optimal value.
3. Dual variable convergence, i.e., $\boldsymbol{\lambda}_p^j(k)$ approaches the dual optimal point $\boldsymbol{\lambda}_p^*(k)$ for all vehicles p.

Proof: The above proposition follows directly from general ADMM convergence properties [22] due to Lemma 1 and Lemma 2 for the distributed platoon problem. $\square$

The convergence of primal feasibility, objective optimality, and dual variables as $j \to \infty$ implies that *1)* individual vehicle solutions are satisfying the coupling collision avoidance constraints (16) and (17); and *2)* global optimality, i.e., cooperative behaviours, is achieved via the local decision-making. In practice, the above convergence is indicated by small primal and dual residuals defined as:

$$r^j(k) = \sum_{p=1}^{n} \left\| \boldsymbol{Z}_p^j(k) - \tilde{\boldsymbol{Z}}_p^j(k) \right\|_2 \leqslant \varepsilon^{\text{pri}}, \qquad (31)$$

$$s^j(k) = \sum_{p=1}^{n} \left\| \tilde{\boldsymbol{Z}}_p^{j+1}(k) - \tilde{\boldsymbol{Z}}_p^j(k) \right\|_2 \leqslant \varepsilon^{\text{dual}}, \qquad (32)$$

where ε^{pri}, $\varepsilon^{\text{dual}}$ are primal and dual feasibility tolerances specified as:

$$\varepsilon^{\text{pri}} = \sqrt{2nN}\varepsilon^{\text{abs}} + \varepsilon^{\text{rel}} \max \left\{ \sum_{p=1}^{n} \left\| \boldsymbol{Z}_p^j(k) \right\|_2, \sum_{p=1}^{n} \left\| \tilde{\boldsymbol{Z}}_p^j(k) \right\|_2 \right\},$$

$$\varepsilon^{\text{dual}} = \sqrt{2nN}\varepsilon^{\text{abs}} + \varepsilon^{\text{rel}} \sum_{p=1}^{n} \left\| \boldsymbol{\lambda}_p^j(k) \right\|_2.$$

Small primal residuals imply that the error trajectories computed locally at *Step 1* and coordinated by the coordinator link at *Step 2* are driven close to each other. Small dual residuals imply that the coordinated error trajectories at *Step 2* are almost constant over iterations.

5   Simulation results and discussions

Simulations are carried out to demonstrate the effectiveness of the proposed cooperative centralized and distributed vehicle platoon controllers. Specifically, we test a platoon with five homogeneous vehicles in a dynamic speed management scenario on a straight way, as illustrated in Figure 2. The platoon is required to track the following dynamic reference speeds broadcast by the roadside link that involve an acceleration and a deceleration:

$$v_0(t) = \begin{cases} 12 \text{ m/s}, & 0 \text{ s} \leq t < 5 \text{ s} \\ 18 \text{ m/s}, & 5 \text{ s} \leq t < 20 \text{ s} \\ 12 \text{ m/s}, & 20 \text{ s} \leq t \leq T \end{cases} \qquad (33)$$

with $T = 30$ s being the total simulation time. The platoon starts at $t = 0$ s with $\boldsymbol{z}_p(0) = [0,0]^T$ for $p = 1, \ldots, 5$. Vehicle physical limits are set as: $v_{\min} = 0$ m/s, $v_{\max} = 22$ m/s, $a_{\min} = -8$ m/s^2, and $a_{\max} = 2$ m/s^2. Vehicle length $L = 5$ m and the desired inter-vehicle distance $d_s = 50$ m. The vehicle reaction time is set as $\tau = 0.8$ s that is larger than the vehicle sampling time $T_s = 0.5$ s. For the MPC controller parameters, we consider a prediction horizon of $N = 10$, and weight matrices $\boldsymbol{Q} = \begin{bmatrix} 10 & 0 \\ 0 & 1 \end{bmatrix}$, $R = 0.1$. ADMM relevant parameters are set as: $\varepsilon^{\text{abs}} = 1\text{e}-3$, $\varepsilon^{\text{rel}} = 1\text{e}-4$ and the augmented Lagrangian parameter $\rho = 1$. Zero initial values of $\boldsymbol{\lambda}_p^0(k)$ and $\tilde{\boldsymbol{Z}}_p^0(k)$ are set for the ADMM iterations. Algorithms are implemented in MATLAB 2016b [30] with solver Cplex [31] on a platform with Intel(R) Core(TM) i3-7100 CPU @3.70 GHz. The controlled platoon performance on maintaining stable safe vehicle formations, and properties of the distributed decision-making are illustrated as follows.

5.1   Safe stable vehicle platoon control

With the dynamic reference speeds in (33), the vehicle platoon needs to maintain the formation by tracking the reference speeds $v_0(t)$ or equivalently, the reference position $s_0(t)$, and keeping the desired inter-vehicle space d_s in a stable and safe way. Figure 3 and Figure 4
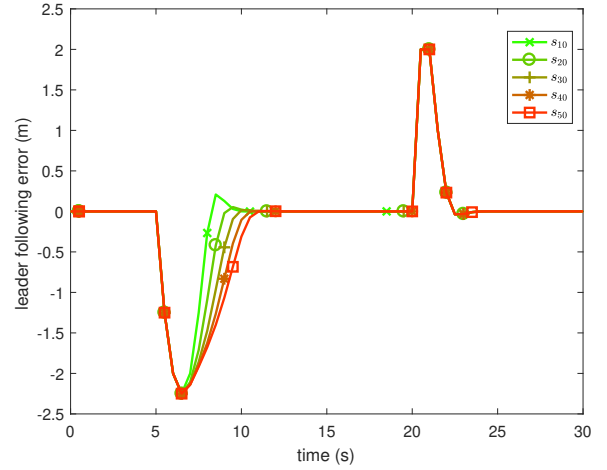

Fig. 3: Reference tracking errors - centralized controller.
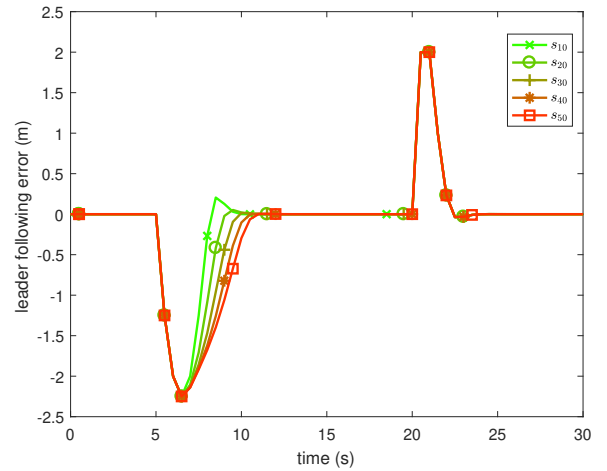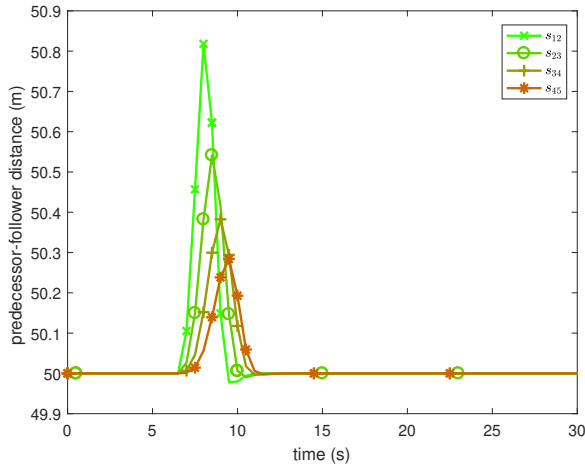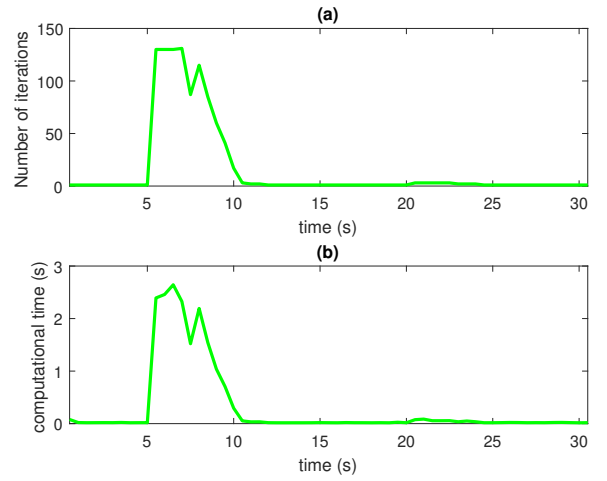

Fig. 4: Reference tracking errors - distributed controllers.

show the reference position tracking errors of all the platoon vehicles by the proposed centralized and distributed controllers, respectively. In both figures, tracking errors are seen for all platoon vehicles when the reference speed changes. However, tracking errors converge to zero in both acceleration (around $t = 5$ s) and deceleration (around $t = 20$ s) cases. Note that variation patterns are slightly different for the acceleration and deceleration periods. Particularly, when the reference speed increases, the magnitude of the deviations from zeros and the time for reaching the steady state of the five platoon vehicles vary from each other. The deviation magnitudes decline and the converging times increase from the platoon start vehicle to the tail vehicle. When the reference speed drops, five vehicles see identical tracking error trajectories. The different patterns during acceleration and deceleration are due to the different activeness of the coupling collision avoidance constraints. The coupling constraints are active during acceleration and inactive during deceleration, as illustrated in Figure 6. Overall, centralized and distributed controllers show similar tracking error trajectories, which also demonstrates that the distributed decision-making achieves global optimality.
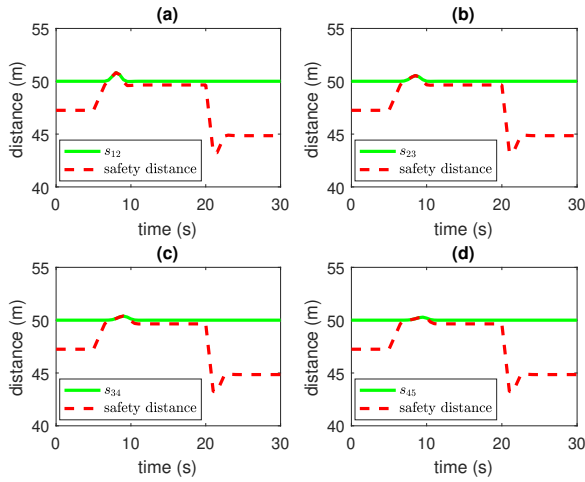
Figure 5 further plots the distances between consecutive vehicles with distributed controllers. Similarly, the predecessor-follower distances fluctuate during the acceleration period and converge to the desired inter-vehicle distance 50 m afterwards. Moreover, the fluctuation magnitude also decreases and the converging time also increases from the platoon head to the tail, which show that the proposed controllers could weaken the deviation or fluctuation impacts along the platoon. Satisfactions of the coupling and local constraints by the distributed controllers are demonstrated in Figure 6 and Figure 7, respectively. In Figure 6, the actual inter-vehicle distances
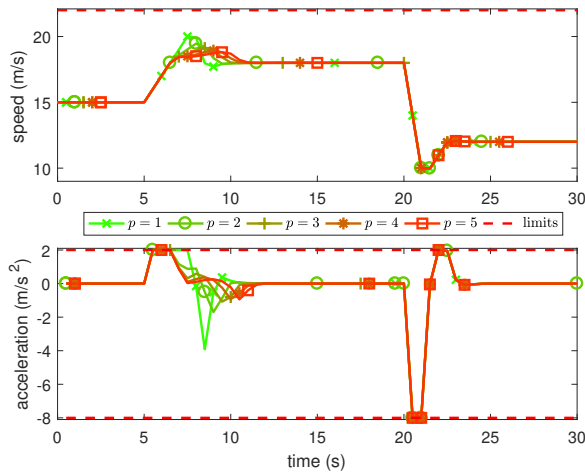
Fig. 5: Inter-vehicle distance.

Fig. 6: Inter-vehicle distances and safety distances.

Fig. 7: Speed and acceleration trajectories.

of all vehicle pairs are not smaller than the safety distance with tight fit showing activeness of the collision avoidance constraints during the acceleration period. Note that the safety distance is not constant due to its dependence on the follower vehicle's speed as in (4). The speed and acceleration trajectories of all vehicles also satisfy the corresponding limits. Fluctuations around the acceleration and deceleration periods and convergence afterwards are also observed in Figure 7.

Fig. 8: Iterations and computational time.

5.2 Convergence of the cooperative distributed controllers

It has been demonstrated that the proposed cooperative distributed controllers can achieve overall system performance and safety. For the defined ADMM convergence accuracy parameters ε^{abs} and ε^{rel}, Figure 8 reports the number of iterations and the corresponding computational times before reaching convergence. The computational times are calculated based on the time required for each iteration and the computational time per iteration sums the maximum time solving the problem at *Step 1* parallelly by all vehicles, the time solving the problems at *Step 2* by the link coordinator, and the dual variable updating time at *Step 3*. The required number of iterations and computational times are relatively large during acceleration due to the activeness of the coupling collision avoidance constraints. Note that the iteration and computational times during deceleration are also larger than those in the steady-state periods since the tracking errors are initialized with zeros for ADMM iterations. Computational complexity is a commonly known issue for iteration based control problems. Although the involved optimizations are all convex, for cases when a large number of iterations are required, timely convergence might not be reached within the sampling time. Then, a reliable decision recovery mechanism needs to be designed for the platoon. Besides, the algorithm efficiency could also be improved by further exploiting the problem structure with designed heuristics such as [24], better tuning controller parameters and using faster computing solvers or platforms.
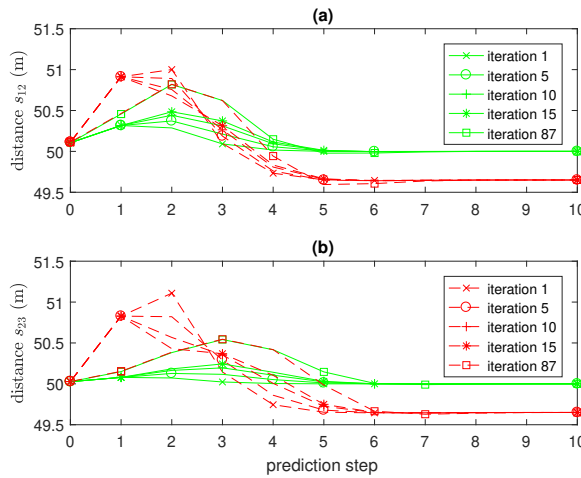
For the convergence behaviours over iterations, we consider a particular time step $k = 14$ after the reference speed increases which involves 87 iterations. As formulated in (31) − (32), the practical convergence of the proposed cooperative distributed controllers for vehicle platoons is indicated by small primal and dual residuals. Figure 9(a) and 9(b) show that both primal and dual residuals decreases rapidly at the first iterations and then converge slowly to the defined accuracy. For comparison, we also implement the centralized controller for the platoon problem at time step $k = 14$. As can be seen in Figure 9(c), the distributed objective value that is the summation of the local objective values of all platoon vehicles at the end of iterations also converges to the centralized optimal value, which illustrates the global optimality convergence. Note that the convergence is achieved from below since the couplings among vehicles are not considered in the local problems. However, by iterative updating the dual variables considering the coordinated trajectories, the cost incurred due to satisfying the collision avoidance constraints are also reflected in distributed objective values in the end.

The iterative communication and coordination procedure for satisfying the coupling constraints is further illustrated in Figure 10 and Figure 11. The iterative inter-vehicle distances (green solid line) are compared with the iterative safety distances (red dashed line) over the prediction horizon. For all consecutive vehicle pairs, the actual

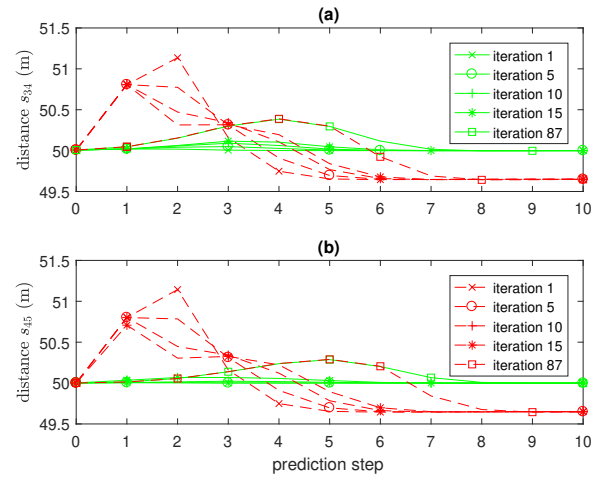**Fig. 9**: Convergence: primal residuals, dual residuals and objectives over iterations at $k = 14$.

Fig. 10: Distance iterations over N at step $k = 14$, green solid line - distance, red dashed line - safety distance. (a) Distances between vehicles 1 and 2; (b) distances between vehicles 2 and 3.

Fig. 11: Distance iterations over N at step $k = 14$, green solid line - distance, red dashed line - safety distance. (a) Distances between vehicles 3 and 4; (b) distances between vehicles 4 and 5.

computation, satisfaction of collision avoidance constraints, and global optimality at the same time with guaranteed convergence. Simulation results in both acceleration and deceleration cases are provided and demonstrate the effectiveness of the proposed controllers for vehicle platoons. Future work will explore more complex vehicle models with relaxed assumptions. Low-level powertrain dynamics and the couplings between longitudinal and lateral vehicle dynamics could be considered in more general ITS scenarios.

Acknowledgement

7 References

1 Wang, M., Daamen, W., Hoogendoorn, S.P., van Arem, B.: 'Potential impacts of ecological adaptive cruise control systems on traffic and environment', *IET Intelligent Transport Systems*, 2014, **8**, (2), pp. 77–86

2 Wang, M., Daamen, W., Hoogendoorn, S.P., van Arem, B.: 'Cooperative car-following control: Distributed algorithm and impact on moving jam features', *IEEE Transactions on Intelligent Transportation Systems*, 2016, **17**, (5), pp. 1459–1471

3 van de Hoef, S., Johansson, K.H., Dimarogonas, D.V.: 'Fuel-efficient en route formation of truck platoons', *IEEE Transactions on Intelligent Transportation Systems*, 2018, **19**, (1), pp. 102–112

4 Sheikholeslam, S., Desoer, C.A.: 'Longitudinal control of a platoon of vehicles with no communication of lead vehicle information: a system level study', *IEEE Transactions on Vehicular Technology*, 1991, **42**, (4), pp. 546–554

5 Zhou, J., Peng, H.: 'Range policy of adaptive cruise control vehicles for improved flow stability and string stability', *IEEE Transactions on Intelligent Transportation Systems*, 2005, **6**, (2), pp. 229–237

6 Xia, Q., Gao, F., Duan, J., He, Y.: 'Decoupled H_∞ control of automated vehicular platoons with complex interaction topologies', *IET Intelligent Transport Systems*, 2017, **11**, (2), pp. 92–101

7 Zheng, Y., Li, S.E., Wang, J., Cao, D., Li, K.: 'Stability and scalability of homogeneous vehicular platoon: Study on the influence of information flow topologies', *IEEE Transactions on Intelligent Transportation Systems*, 2015, **17**, (1), pp. 14–26

8 Guo, G., Yue, W.: 'Hierarchical platoon control with heterogeneous information feedback', *IET Control Theory & Applications*, 2011, **5**, (15), pp. 1766–1781

9 Wei, Y., Wang, L., Ge, G.: 'Event-triggered platoon control of vehicles with time-varying delay and probabilistic faults', *Mechanical Systems & Signal Processing*, 2017, **87**, pp. 96–117

10 Bernardo, M.D., Salvi, A., Santini, S.: 'Distributed consensus strategy for platooning of vehicles in the presence of time-varying heterogeneous communication delays', *IEEE Transactions on Intelligent Transportation Systems*, 2015, **16**, (1), pp. 102–112

11 Hounsell, N.B., Shrestha, B.P., Piao, J., McDonald, M.: 'Review of urban traffic management and the impacts of new vehicle technologies', *IET Intelligent Transport Systems*, 2009, **3**, (4), pp. 419–428

inter-vehicle distances are below the safety distances for the first iterations over certain prediction steps. However, as iterations increase, the green solid lines are pulled up from below while the red dashed lines are pulled down from above. Upon reaching convergence, the inter-vehicle distances coincide with or are above the safety distances over all prediction steps, which is consistent with Figure 6. The convergence pattern is because the platoon vehicles are solving local problems selfishly with the goal mainly on maintaining desired vehicle spaces. Along with iterations, the goal is driven also to satisfy the safety constraints by updating dual variables. Convergence of primal and dual residuals imply that the optimal trade-off between local and coupling goals is achieved resulting in overall optimality.

6 Conclusions and future research

We consider intelligent vehicle platoon problems in the context of dynamic speed management scenarios in this paper. Cooperative predictive controllers are proposed to maintain the vehicle platoon formations and track dynamic reference speeds in a stable and safe way. Both centralized and distributed decision-making solutions are proposed with guaranteed closed-loop stability. Particularly for the distributed controllers, only vehicle-to-infrastructure communications are required, which differs from the existing approaches that mostly necessitate certain types of vehicle-to-vehicle communications. Moreover, the distributed controllers ensure parallel local

12 Hao, H., Barooah, P.: 'Stability and robustness of large platoons of vehicles with double-integrator models and nearest neighbor interaction', *International Journal of Robust and Nonlinear Control*, 2013, **23**, (18), pp. 2097–2122

13 Gong, S., Shen, J., Du, L.: 'Constrained optimization and distributed computation based car following control of a connected and autonomous vehicle platoon', *Transportation Research Part B: Methodological*, 2016, **94**, pp. 314–334

14 Mayne, D.Q.: 'Model predictive control: Recent developments and future promise', *Automatica*, 2014, **50**, (12), pp. 2967 – 2986

15 Dunbar, W.B., Caveney, D.S.: 'Distributed receding horizon control of vehicle platoons: Stability and string stability', *IEEE Transactions on Automatic Control*, 2012, **57**, (3), pp. 620–633

16 Zheng, Y., Li, S.E., Li, K., Borrelli, F., Hedrick, J.K.: 'Distributed model predictive control for heterogeneous vehicle platoons under unidirectional topologies', *IEEE Transactions on Control Systems Technology*, 2017, **25**, (3), pp. 899–910

17 Keviczky, T., Borrelli, F., Fregene, K., Godbole, D., Balas, G.J.: 'Decentralized receding horizon control and coordination of autonomous vehicle formations', *IEEE Transactions on Control Systems Technology*, 2008, **16**, (1), pp. 19–33

18 Maestre, J.M., Negenborn, R.R.: 'Distributed Model Predictive Control Made Easy'. (Dordrecht, The Netherlands: Springer, 2014)

19 Dunbar, W.B., Murray, R.M.: 'Distributed receding horizon control for multi-vehicle formation stabilization', *Automatica*, 2006, **42**, (4), pp. 549–558

20 Richards, A., How, J.P.: 'Robust distributed model predictive control', *International Journal of Control*, 2007, **80**, (9), pp. 1517–1531

21 Jia, D., Krogh, B. 'Min-max feedback model predictive control for distributed control with communication'. In: Proceedings of the 2002 American Control Conference (ACC). (Anchorage, USA, 2002. pp. 4507–4512

22 Boyd, S., Parikh, N., Chu, E., Peleato, B., Eckstein, J.: 'Distributed optimization and statistical learning via the alternating direction method of multipliers', *Foundations and Trends in Machine Learning*, 2011, **3**, (1), pp. 1–122

23 Farokhi, F., Shames, I., Johansson, K.H. 'Distributed MPC via dual decomposition and alternative direction method of multipliers'. In: Maestre, J.M., Negenborn, R.R., editors. Distributed Model Predictive Control Made Easy. (Springer, 2014. pp. 115–131

24 Mota, J.F., Xavier, J.M., Aguiar, P.M., Puschel, M. 'Distributed ADMM for model predictive control and congestion control'. In: Proceedings of 51st Annual Conference on Decision and Control. (Maui, USA: IEEE, 2012. pp. 5110–5115

25 Hao, Y.O., Gerdes, J.C. 'Cooperative collision avoidance via proximal message passing'. In: Proceedings of American Control Conference. (Chicago, USA, 2015. pp. 4124–4130

26 Zheng, H., Negenborn, R.R., Lodewijks, G.: 'Fast ADMM for distributed model predictive control of cooperative waterborne AGVs', *IEEE Transactions on Control Systems Technology*, 2017, **25**, (4), pp. 1406 – 1413

27 Ma, Y., Chen, J., Peng, Y., Wang, T. 'Simultaneous lateral stability and energy efficiency control of over-actuated electric vehicles'. In: Proceedings of American Control Conference. (Milwaukee, USA, in press, 2018.

28 Li, S.E., Zheng, Y., Li, K., Wu, Y., Hedrick, J.K., Gao, F., et al.: 'Dynamical modeling and distributed control of connected and automated vehicles: Challenges and opportunities', *IEEE Intelligent Transportation Systems Magazine*, 2017, **9**, (3), pp. 46–58

29 Kerrigan, E.C. 'Robust Constraint Satisfaction: Invariant Sets and Predictive Control'. University of Cambridge. Cambridge, UK, 2000

30 MATLAB: 'R2016b'. (Natick, Massachusetts: The MathWorks Inc., 2016)

31 ILOG. 'IBM ILOG CPLEX Optimizer'. (, 2010. Available from: http://www-01.ibm.com/software/integration/optimization/cplex-optimizer/